Closed-Form Inverse Kinematic Joint Solution for Humanoid Robots

Muhammad A. Ali, H. Andy Park, and C. S. George Lee

Abstract— This paper focuses on developing a consistent methodology for deriving a closed-form inverse kinematic joint solution of a general humanoid robot. Most humanoid-robot researchers resort to iterative methods for inverse kinematics using the Jacobian matrix to avoid the difficulty of finding a closed-form joint solution. Since a closed-form joint solution, if available, has many advantages over iterative methods, we have developed a novel reverse decoupling mechanism method by viewing the kinematic chain of a limb of a humanoid robot in reverse order and then decoupling it into the positioning and orientation mechanisms, and finally utilizing the inverse transform technique in deriving a consistent joint solution for the humanoid robot. The proposed method presents a simple and efficient procedure for finding the joint solution for most of the existing humanoid robots. Extensive computer simulations of the proposed approach on a Hubo KHR-4 humanoid robot show that it can be applied easily to most humanoid robots with slight modifications.

Index Terms— Reverse Decoupling Method, Inverse Kinematics, Inverse Transform

I. INTRODUCTION

A humanoid robot is a multi-jointed mechanism that mechanically emulates a human's functions, movements and activities. It can be considered as a biped robot with an upper main body, linking two arms, a neck and a head, or as a combination of multiple manipulators, which are themselves linked together through waist and neck joints to emulate a human's functions. Because of its human-like, bipedal movement, the kinematic structure of a humanoid robot has no fixed root node and has a large number of degree-of-freedom (DOF). Since the robot servo system requires the reference inputs to be in joint coordinates and a task is generally stated in the Cartesian coordinate system, controlling the position and orientation of the end point of a limb (an arm or a leg) of a humanoid robot requires the understanding of the inverse kinematic joint solution of a humanoid robot.

Pieper outlined two conditions for finding a closed-form joint solution to a robot manipulator in which either three adjacent joint axes are parallel to one another or they intersect at a single point [1]. Although a robot manipulator may satisfy one of these two conditions for finding the closed-form joint solution, it is difficult to develop a consistent procedure for finding a closed-form joint solution for a

humanoid robot and selecting one desirable solution from multiple solutions.

Most humanoid-robot researchers often use iterative methods for controlling humanoid robots [2], [3], [4]. One of the iterative methods makes use of the Jacobian matrix [2], [5]. Singularity, redundancy, and computational complexity are the main drawbacks of using the inverse-Jacobian-matrix approach [4]. Since the Jacobian method is velocity based instead of being position based, significant accumulation of error in position can result due to the iterative nature of the algorithm. Furthermore, the Jacobian matrix is singular when a limb of the humanoid robot is in a fully stretched condition. De Angulo et al [6] suggested learning the inverse kinematics to tackle with some of the drawbacks of the Jacobian method.

Another commonly adopted method for inverse kinematics is the geometric method [7], [8], [9]. However, the geometric method requires geometric intuition in solving the joint solution of a manipulator, and it may become more difficult to obtain the joint solution when more than four or five joints are involved. Furthermore, it is difficult to generalize the approach from one humanoid robot to another. In [10], [11], a closed-form solution for a 7-DOF humanoid arm was obtained but it was done by dividing the inverse kinematics problem into smaller sub-problems using the constraint on the elbow position. This paper presents a general closed-form joint solution with decision equations to select a proper solution from multiple solutions.

Another method, called the inverse-transform technique, was presented by Paul et al [12] to obtain the inverse kinematic joint solution of a 6-DOF robot manipulator. Cui et al [13] derived a closed-form joint solution for a 6-DOF humanoid robot arm but only the solution of joint angles within a certain range was considered and the singularities were not discussed. In this paper, we propose a novel reverse decoupling mechanism method by viewing the kinematic chain of a limb of a humanoid robot in reverse order and then decoupling it into the positioning and orientation mechanisms, and finally utilizing the inverse transform technique in deriving a consistent joint solution for the humanoid robot. We have also obtained the decision equations that identify the correct joint solution from multiple solutions. The proposed approach is applied to a Hubo KHR-4 humanoid robot, and the proposed technique can also be applied to an ASIMO robot from Honda Motors, an HRP-2 robot from Kawada Industries, and a HOAP-2 robot from Fujitsu Automation with slight modifications. Computer simulations were performed to verify the correctness of the closed-form inverse kinematic joint solutions for these humanoid robots.

Muhammad A. Ali, Hyungju Andy Park, and C. S. George Lee are with the School of Electrical and Computer Engineering, Purdue University, West Lafayette, IN 47907, USA. {ali2, andypark, csglee}@purdue.edu

II. KINEMATIC LINK COORDINATE FRAMES

We shall use the Denavit-Hartenberg (D-H) matrix representation [14] for each link to describe the rotational and translational relationship between adjacent links. Using the D-H matrix representation and following the link coordinate frame assignment outlined in [7], one can assign link coordinate frames that are consistent with the positive direction of rotation of joints of a humanoid robot. A Hubo robot (see Fig. 1 and Table I) is used as an example in our discussion.
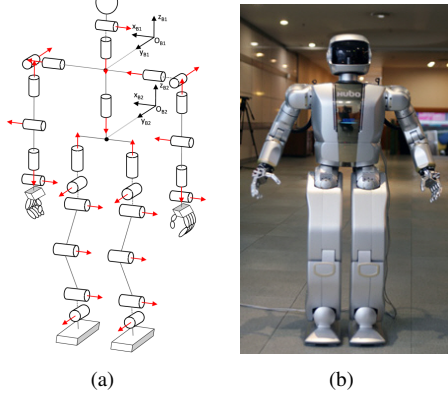

(a) (b)

Fig. 1. A Hubo KHR-4 Humanoid Robot.

TABLE I
DEGREES OF FREEDOM OF A HUBO KHR-4 HUMANOID ROBOT

Head	Waist	Arm	Hand	Leg	Total
2/Neck	1/Waist	3/Shoulder	5/Hand	3/Hip	
2/Eyes		1/Elbow		1/Knee	
		2/Wrist		2/Ankle	
6 DOF	1 DOF	12 DOF	10 DOF	12 DOF	41 DOF

We first establish two base coordinate frames B1 and B2 for the Hubo KHR-4 humanoid robot. B1 is established at the center of the neck and is the reference coordinate frame for the arms and the head, and B2 is the reference coordinate frame for the legs. B2 is linked to B1 through a waist joint, and there is a simple link transformation matrix between B1 and B2. As a result, B1 is considered to be the global base coordinate frame for the whole robot.

Since the general kinematic structures of the left arm/leg of a Hubo KHR-4 robot are identical to those of the right arm/leg, we have assigned identical coordinate frames for the left and right limbs. Figures 2 and 3 show the assigned link coordinate frames and their D-H parameters for the right arm and the right leg, respectively. From the established link coordinate frames and the D-H parameters, the position and orientation of the end-effector of a limb can be obtained by chain-multiplying the 6 link-transformation matrices together to obtain the spatial displacement of the 6th coordinate frame with respect to the base/reference coordinate frame:

$$ {}^0\mathbf{T}_6 = \prod_{i=1}^{6} {}^{i-1}\mathbf{A}_i = {}^0\mathbf{A}_1\,{}^1\mathbf{A}_2\,{}^2\mathbf{A}_3\,{}^3\mathbf{A}_4\,{}^4\mathbf{A}_5\,{}^5\mathbf{A}_6 $$

$$ = \begin{bmatrix} \mathbf{x}_6 & \mathbf{y}_6 & \mathbf{z}_6 & \mathbf{p}_6 \\ 0 & 0 & 0 & 1 \end{bmatrix} = \begin{bmatrix} \mathbf{n} & \mathbf{s} & \mathbf{a} & \mathbf{p} \\ 0 & 0 & 0 & 1 \end{bmatrix} \quad (1) $$

where $\mathbf{x}_i$, $\mathbf{y}_i$, and $\mathbf{z}_i$ represent the unit vectors along the principal axes of the coordinate frame i, ${}^{i-1}\mathbf{A}_i$ is a general
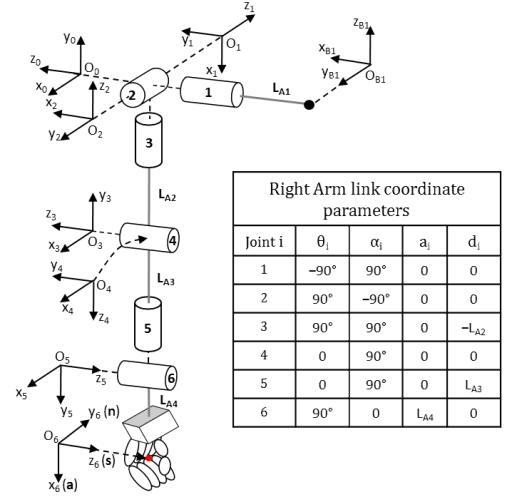
Fig. 2. Link Coordinate Frames of the Right Arm of a Hubo KHR-4 Robot and its D-H Parameters.

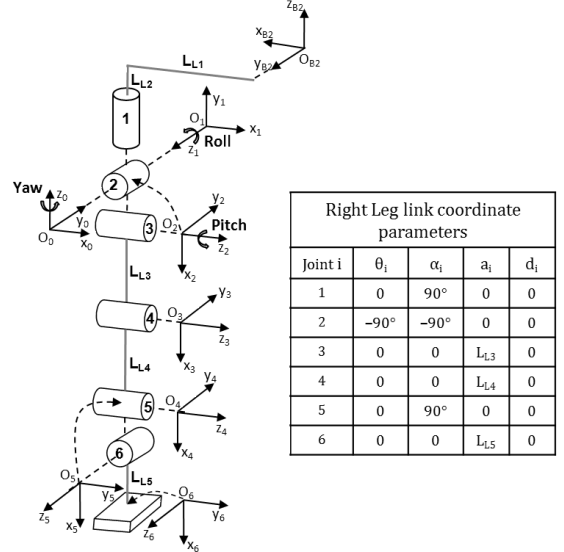| Right Arm link coordinate parameters			
Joint i	θ_i	α_i	a_i	d_i
1	−90°	90°	0	0
2	90°	−90°	0	0
3	90°	90°	0	$-L_{A2}$
4	0	90°	0	0
5	0	90°	0	L_{A3}
6	90°	0	L_{A4}	0

Fig. 3. Link Coordinate Frames of the Right Leg of a Hubo KHR-4 Robot and its D-H Parameters.

Right Leg link coordinate parameters			
Joint i	θ_i	α_i	a_i	d_i
1	0	90°	0	0
2	−90°	−90°	0	0
3	0	0	L_{L3}	0
4	0	0	L_{L4}	0
5	0	90°	0	0
6	0	0	L_{L5}	0

link transformation matrix, relating the ith coordinate frame to the $(i-1)$th coordinate frame, and $[\mathbf{n}, \mathbf{s}, \mathbf{a}, \mathbf{p}]$ represents the normal vector, the sliding vector, the approach vector, and the position vector of the hand, respectively [7]. This forward kinematic equation will be used in deriving the closed-form joint solution for a Hubo robot.

III. INVERSE KINEMATIC JOINT SOLUTION

Given the desired position and orientation of the end-effector of a limb (an arm or a leg) and the geometric link parameters with respect to a reference coordinate system, the inverse kinematic position problem is to find a closed-form joint solution for positioning the end-effector with the desired position and orientation. And if a closed-form joint solution exists, then it is desirable to determine how many different joint solutions will satisfy the same condition. If a limb of the robot has six joints, we should, in principle, be able to find a closed-form joint solution. A joint solution is said to be "closed-form" if the unknown joint angles can be

solved for symbolically in terms of the arc-tangent function.

Looking at some existing humanoid robots shown in Fig. 4, we note all of them have limbs with at most six joints. Hence, one should be able to find closed-form solutions for these robots, and since the kinematic configuration of all these humanoid robots is almost the same as a Hubo robot, the developed closed-form joint solution will be applicable to these humanoid robots with only slight modifications.

(a)   (b)   (c)

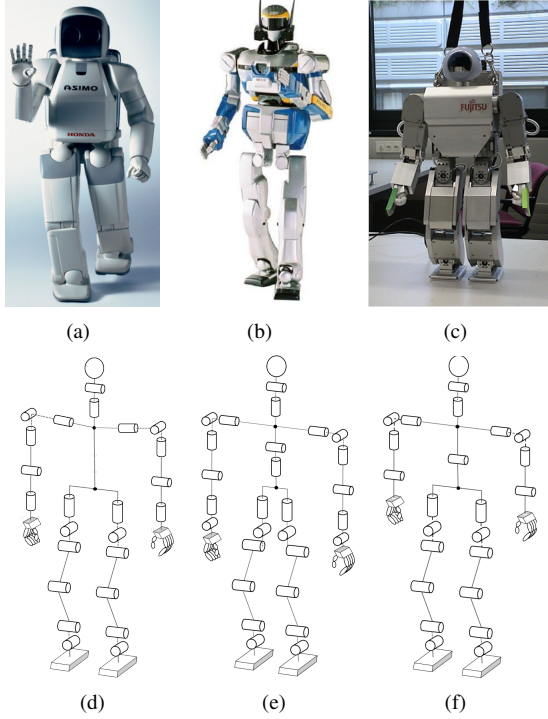(d)   (e)   (f)

Fig. 4.   (a) HONDA ASIMO Robot and its associated kinematic diagram in (d), (b) AIST HRP-2 Robot and its associated kinematic diagram in (e), and (c) Fujitsu HOAP-2 Robot and its associated kinematic diagram in (f).

In tackling the inverse kinematic position problem, Pieper indicated a closed-form joint solution exists if a robot manipulator's three adjacent joint axes are parallel to one another or they intersect at a single point [1]. Considering a limb in which the joint axes of the last three joints intersect at a point, the position vector $\mathbf{p}$ to the wrist coordinate frame decouples the limb into positioning and orientation subsystems, and obviously it is a function of just the first three joint angles; the last three joint angles contribute nothing to the position but the orientation. Hence, there are three equations with known variables p_x, p_y and p_z and three unknown joint angles θ_1, θ_2 and θ_3. The last three joint angles are determined from $[\mathbf{n}, \mathbf{s}, \mathbf{a}]$ and the solved first three joint angles. The key concept here is that the robot is decoupled with the three of the six joint angles for positioning and three joint angles for orientation.

Unfortunately, for the limbs of the existing humanoid robots, the joint axes of the last three joints do not intersect at a point; for example, the last three joint axes of the right leg/arm of a Hubo robot do not intersect at a point. As a result, the position vector $\mathbf{p}$ is a function of four joint angles θ_1, θ_2, θ_3, and θ_4. Hence, obtaining a closed-form joint solution becomes complicated, if not impossible. However,

a closer examination reveals that the joint axes of the first three joints do intersect at a point. This means that if we view the IK-problem with the joint angles in reverse order; that is, with the position/orientation of the base coordinate frame referenced to the end-effector coordinate frame, the new position vector, denoted as $\mathbf{p}'$, is a function of only the three joint angles θ_4, θ_5 and θ_6. This new position vector $\mathbf{p}'$ decouples the limb into positioning and orientation subsystems. To solve the IK-problem in this reverse way, we take the inverse of both sides of Eq. (1) so that the new composite link transformation matrix $\mathbf{T}'$ is now referenced to the end-effector coordinate frame; that is,

$$\mathbf{T}' = \begin{bmatrix} \mathbf{n} & \mathbf{s} & \mathbf{a} & \mathbf{p} \\ 0 & 0 & 0 & 1 \end{bmatrix}^{-1} = \begin{bmatrix} \mathbf{n}' & \mathbf{s}' & \mathbf{a}' & \mathbf{p}' \\ 0 & 0 & 0 & 1 \end{bmatrix}$$

$$= {}^6\mathbf{A}_5{}^5\mathbf{A}_4{}^4\mathbf{A}_3{}^3\mathbf{A}_2{}^2\mathbf{A}_1{}^1\mathbf{A}_0 = {}^6\mathbf{A}_0 \qquad (2)$$

Thus, the novelty here is to observe the intersection of 3 adjacent joint axes in the kinematic chain for decoupling the robotic arm/leg system into positioning and orientation subsystems for solving its joint solution. We shall next show how this reverse decoupling method can be applied to a Hubo robot for finding its joint solution and extend it to other humanoid robots shown in Fig. 4.

A. Joint Solution for the Right Leg of a Hubo Robot

The transformation matrix from the base coordinate frame B2 attached to the waist to the first coordinate frame of the right leg is

$$ {}^{B2}\mathbf{A}_0 = \begin{bmatrix} -1 & 0 & 0 & l_{L1} \\ 0 & -1 & 0 & 0 \\ 0 & 0 & 1 & -l_{L2} \\ 0 & 0 & 0 & 1 \end{bmatrix} \qquad (3)$$

To obtain the solution for the last three joint angles θ_4, θ_5 and θ_6, we equate the elements of the position vector $\mathbf{p}'$ in both sides of Eq. (2) as

$$-C_6(C_{45}l_{L3} + C_5l_{L4}) = p'_x + l_{L5} \qquad (4)$$

$$S_6(C_{45}l_{L3} + C_5l_{L4}) = p'_y \qquad (5)$$

$$-S_{45}l_{L3} - S_5l_{L4} = p'_z \qquad (6)$$

where $S_i \equiv \sin\theta_i, C_i \equiv \cos\theta_i$, $S_{ij} \equiv \sin(\theta_i + \theta_j)$, $C_{ij} \equiv \cos(\theta_i + \theta_j)$, and l_{Li} are geometric link parameters in Fig. 3. It is evident that these three equations have three unknowns θ_4, θ_5 and θ_6. By squaring and adding these three equations, we can obtain C_4 and then S_4 from C_4, and from which we can solve for the joint solution θ_4,

$$C_4 = \frac{(p'_x + l_{L5})^2 + p'^2_y + p'^2_z - l^2_{L3} - l^2_{L4}}{2l_{L3}l_{L4}}$$

$$\theta_4 = \operatorname{atan2}(\pm\sqrt{1 - C_4^2}, C_4) \qquad (7)$$

where $\operatorname{atan2}(y, x)$ is an arc-tangent function, which returns $\tan^{-1}(\frac{y}{x})$ adjusted to the proper quadrant. By squaring Eqs. (4) and (5), adding and expanding them, we get

$$C_5(C_4l_{L3} + l_{L4}) - S_4S_5l_{L3} = \pm\sqrt{(p'_x + l_{L5})^2 + p'^2_y} \qquad (8)$$

By expanding Eq. (6), we obtain

$$S_5(C_4l_{L3} + l_{L4}) + C_5(S_4l_{L3}) = -p'_z \qquad (9)$$

Let $C_4 l_{L3} + l_{L4} = rC_\psi$ and $S_4 l_{L3} = rS_\psi$, and substituting them into Eqs. (8) and (9), we get, correspondingly,

$$rC_{5\psi} = \pm\sqrt{(p'_x + l_{L5})^2 + p'^2_y} \qquad (10)$$

$$rS_{5\psi} = -p'_z \qquad (11)$$

where $r = \sqrt{(p'_x + l_{L5})^2 + p'^2_y + p'^2_z}$ and $\psi = $ atan2$(S_4 l_{L3}, C_4 l_{L3} + l_{L4})$. Dividing Eq. (11) by Eq. (10), we obtain $\tan(\theta_5 + \psi)$, which finally gives the joint solution for θ_5,

$$\theta_5 = \text{atan2}\left(-p'_z, \pm\sqrt{(p'_x + l_{L5})^2 + p'^2_y}\right) - \psi \qquad (12)$$

Dividing Eq. (5) by Eq. (4), we get the joint solution for θ_6,

$$\theta_6 = \text{atan2}\left(p'_y, -p'_x - l_{L5}\right) \qquad (13)$$

and if $C_{45} l_{L3} + C_5 l_{L4} < 0$, then we have $\theta_6 = \theta_6 + \pi$.

To obtain the other three joint angles θ_1, θ_2 and θ_3, we can use the inverse transform method [12] by moving the link transformation matrix $^6\mathbf{A}_5$ to the left-hand side of Eq. (2). This results in a matrix equation that we label as G_2 equation. The left-hand side of G_2 is,

$$G_{2-leg}^{(LHS)} = {}^5\mathbf{A}_6 \begin{bmatrix} \mathbf{n}' & \mathbf{s}' & \mathbf{a}' & \mathbf{p}' \\ 0 & 0 & 0 & 1 \end{bmatrix} =$$

$$\begin{bmatrix} C_6 n'_x - S_6 n'_y, & C_6 s'_x - S_6 s'_y, & C_6 a'_x - S_6 a'_y, & C_6 p'_x - S_6 p'_y + C_6 l_{L5} \\ S_6 n'_x + C_6 n'_y, & S_6 s'_x + C_6 s'_y, & S_6 a'_x + C_6 a'_y, & S_6 p'_x + C_6 p'_y + S_6 l_{L5} \\ n'_z, & s'_z, & a'_z, & p'_z \\ 0 & 0 & 0 & 1 \end{bmatrix}$$

and the right-hand side of G_2 is,

$$G_{2-leg}^{(RHS)} = {}^5\mathbf{A}_0 = {}^5\mathbf{A}_4{}^4\mathbf{A}_3{}^3\mathbf{A}_2{}^2\mathbf{A}_1{}^1\mathbf{A}_0 =$$

$$\begin{bmatrix} C_1 C_2 C_{345} - S_1 S_{345}, & S_1 C_2 C_{345} + C_1 S_{345}, & S_2 C_{345}, & -C_{45} l_{L3} - C_5 l_{L4} \\ -C_1 S_2, & -S_1 S_2, & C_2, & 0 \\ C_1 C_2 S_{345} + S_1 C_{345}, & S_1 C_2 S_{345} - C_1 C_{345}, & S_2 S_{345}, & -S_{45} l_{L3} - S_5 l_{L4} \\ 0 & 0 & 0 & 1 \end{bmatrix}$$

By comparing the elements (2,3) of the LHS and RHS of G_2, we can find C_2 and S_2, and from which we obtain the joint solution for θ_2

$$\theta_2 = \text{atan2}\left(\pm\sqrt{1 - (S_6 a'_x + C_6 a'_y)^2}, S_6 a'_x + C_6 a'_y\right) \qquad (14)$$

By comparing the elements (2,1) and (2,2) of the LHS and RHS of G_2, we get two equations from these two elements,

$$S_1 S_2 = -S_6 s'_x - C_6 s'_y \quad \text{and} \quad C_1 S_2 = -S_6 n'_x - C_6 n'_y$$

By dividing these two equations, we obtain the joint solution for θ_1,

$$\theta_1 = \text{atan2}\left(-S_6 s'_x - C_6 s'_y, -S_6 n'_x - C_6 n'_y\right) \qquad (15)$$

and if $S_2 < 0$, then $\theta_1 = \theta_1 + \pi$.

By comparing the elements (1,3) and (3,3) of the LHS and RHS of G_2, we get two equations in S_{345} and C_{345}, and by dividing these two equations, we find the joint angle θ_{345}, $\quad S_2 S_{345} = a'_z \quad$ and $\quad S_2 C_{345} = C_6 a'_x - S_6 a'_y$

$$\theta_{345} = \text{atan2}\left(a'_z, C_6 a'_x - S_6 a'_y\right) \qquad (16)$$

and if $S_2 < 0$, then we have $\theta_{345} = \theta_{345} + \pi$. Finally, from Eq. (16), we can find the joint solution θ_3

$$\theta_3 = \theta_{345} - \theta_4 - \theta_5 \qquad (17)$$

The above closed-form joint solution can be easily applied to the left leg by replacing $+l_{L1}$ with $-l_{L1}$ in Eq. (3). We should mention that for the legs, singularity due to two collinear joint axes does not exist within the valid joint-angle constraints.

B. Joint Solution for the Right Arm of a Hubo Robot

The transformation matrix from the base coordinate frame $B1$ attached to the neck to the first coordinate frame of the right arm is,

$$^{B1}\mathbf{A}_0 = \begin{bmatrix} 0 & 0 & 1 & l_{A1} \\ 1 & 0 & 0 & 0 \\ 0 & 1 & 0 & 0 \\ 0 & 0 & 0 & 1 \end{bmatrix} \qquad (18)$$

Next, we obtain G_2 for the right arm using the inverse transform method,

$$G_{2-arm}^{(LHS)} = \begin{bmatrix} g_{211} & g_{212} & g_{213} & C_6(p'_x + l_{A4}) - S_6 p'_y \\ g_{221} & g_{222} & g_{223} & S_6(p'_x + l_{A4}) + C_6 p'_y \\ g_{231} & g_{232} & g_{233} & p'_z \\ 0 & 0 & 0 & 1 \end{bmatrix}$$

$$G_{2-arm}^{(RHS)} = \begin{bmatrix} g_{211} & g_{212} & g_{213} & S_4 C_5 l_{A2} \\ g_{221} & g_{222} & g_{223} & -C_4 l_{A2} - l_{A3} \\ g_{231} & g_{232} & g_{233} & S_4 S_5 l_{A2} \\ 0 & 0 & 0 & 1 \end{bmatrix}$$

By comparing the elements (1,4), (2,4) and (3,4) of the LHS and RHS of G_2, we have

$$C_6(p'_x + l_{A4}) - S_6 p'_y = S_4 C_5 l_{A2} \qquad (19)$$

$$S_6(p'_x + l_{A4}) + C_6 p'_y = -C_4 l_{A2} - l_{A3} \qquad (20)$$

$$p'_z = S_4 S_5 l_{A2} \qquad (21)$$

Let $p'_x + l_{A4} = rC_\psi$ and $p'_y = rS_\psi$, and substituting them into Eqs. (19), (20) and (21), we get, correspondingly,

$$rC_{6\psi} = S_4 C_5 l_{A2} \qquad (22)$$

$$rS_{6\psi} = -C_4 l_{A2} - l_{A3} \qquad (23)$$

$$p'_z = S_4 S_5 l_{A2} \qquad (24)$$

where $r = \sqrt{(p'_x + l_{A4})^2 + (p'_y)^2}$ and $\psi = $ atan2$(p'_y, p'_x + l_{A4})$. By squaring Eqs. (22), (23), and (24) and adding them up, we can obtain C_4 and then S_4 from C_4, and from which we can find the joint solution for θ_4,

$$C_4 = \frac{(p'_x + l_{A4})^2 + p'^2_y + p'^2_z - l^2_{A2} - l^2_{A3}}{2 l_{A2} l_{A3}}$$

$$\theta_4 = \text{atan2}(\pm\sqrt{1 - C^2_4}, C_4). \qquad (25)$$

From Eq. (24), we can find S_5 and then C_5, and from which we can find the joint solution θ_5,

$$S_5 = p'_z/(S_4 l_{A2}); \quad \theta_5 = \text{atan2}(S_5, \pm\sqrt{1 - S^2_5}). \qquad (26)$$

By dividing Eq. (23) by Eq. (22), we get

$$\tan(6\psi) = \tan(\theta_6 + \psi) = \frac{S_{6\psi}}{C_{6\psi}} = \frac{-C_4 l_{A2} - l_{A3}}{S_4 C_5 l_{A2}} \qquad (27)$$

and from which we obtain the joint solution θ_6,

$$\theta_6 = \text{atan2}(-(C_4 l_{A2} + l_{A3}), S_4 C_5 l_{A2}) - \psi. \qquad (28)$$

For the solution of the rest of the joints, we use G_4,

$$G_{4-arm}^{(LHS)} = \begin{bmatrix} g_{411} & g_{412} & g_{413} & g_{414} \\ g_{421} & g_{422} & g_{423} & g_{424} \\ g_{431} & g_{432} & g_{433} & g_{434} \\ 0 & 0 & 0 & 1 \end{bmatrix}$$

$$G_{4-arm}^{(RHS)} = \begin{bmatrix} C_1C_2C_3 - S_1S_3 & C_1S_3 + S_1C_2C_3 & S_2C_3 & 0 \\ -C_1S_2 & -S_1S_2 & C_2 & l_{A2} \\ S_1C_3 + C_1C_2S_3 & S_1C_2S_3 - C_1C_3 & S_2S_3 & 0 \\ 0 & 0 & 0 & 1 \end{bmatrix}$$

By comparing the element (2,3) of LHS and RHS of G_4, we get C_2 and then S_2, and the joint solution θ_2 from them,

$$C_2 = g_{423} = a_z'S_4S_5 - a_y'(C_4C_6 + S_4C_5S_6)$$
$$- a_x'(C_4S_6 - S_4C_5C_6)$$
$$\theta_2 = \text{atan2}(\pm\sqrt{1 - C_2^2}, C_2). \qquad (29)$$

By comparing the elements (1,3) and (3,3) of LHS and RHS of G_4, we get two equations. By dividing these two equations, we can find the joint solution θ_3,

$$g_{413} = a_x'(C_4C_5C_6 + S_4S_6) + C_4S_5a_z' + (S_4C_6 - C_4C_5S_6)a_y'$$
$$g_{433} = S_5C_6a_x' - C_5a_z' - S_5S_6a_y'$$
$$\theta_3 = \text{atan2}(g_{433}, g_{413}), \qquad (30)$$

and if $S_2 < 0$, then $\theta_3 = \theta_3 + \pi$. By comparing the elements (2,1) and (2,2) of LHS and RHS of G_4, we get two equations. By dividing these two equations, we find the joint angle θ_1,

$$g_{421} = (S_4C_5C_6 - C_4S_6)n_x' + S_4S_5n_z' - (S_4C_5S_6 + C_4C_6)n_y'$$
$$g_{422} = (S_4C_5C_6 - C_4S_6)s_x' + S_4S_5s_z' - (S_4C_5S_6 + C_4C_6)s_y'$$
$$\theta_1 = \text{atan2}(-g_{422}, -g_{421}), \qquad (31)$$

and if $S_2 < 0$, then $\theta_1 = \theta_1 + \pi$.

The above closed-form joint solution can be applied to the left arm with $-l_{A1}$ instead of $+l_{A1}$ in Eq. (18).

In the above joint solution for the right leg and arm of a Hubo robot, we see each of θ_2, θ_4 and θ_5 have two solutions, yielding a total of 8 possible solutions. We shall discuss these multiple solutions in subsection III-D. When the specified position/orientation is out of range of the arm or leg, the joint values obtained from the above equations will have imaginary parts, indicating that no real solution exists.

C. Singularities with Collinear Joint Axes in the Arm

We have identified three cases of singularity that arise within the joint-limit constraints. They all occur when one joint axis aligns with another joint axis, thus reducing the number of degrees of freedom by one.

Case 1: When $\theta_2 = \pi$, the joint-three axis aligns with the joint-one axis, resulting in a singularity. In this case, the sum of the joint angles $\theta_T = \theta_1 + (-\theta_3)$ is found using elements (2,1) and (2,2) of LHS and RHS of G_2 with $\theta_2 = \pi$,

$$\theta_T = \text{atan2}(-C_6s_y' - S_6s_x', -C_6n_y' - S_6n_x'),$$

and if $S_4 < 0$, then $\theta_T = \theta_T + \pi$. To determine θ_1 and θ_3 from θ_T, we can keep the current value of θ_1 unchanged, and θ_3 is evaluated from θ_T as $\theta_3 = \theta_1 - \theta_T$.

Case 2: When $\theta_4 = 0$, the joint-five axis aligns with the joint-three axis, which results in a singularity. In this

case, the sum of the joint angles $\theta_T = \theta_3 - \theta_5$ is found using elements (1,3) and (3,3) of LHS and RHS of G_2 with $\theta_4 = 0$,

$$\theta_T = \text{atan2}(-a_z', a_x'C_6 - a_y'S_6)$$

and if $S_2 < 0$, then $\theta_T = \theta_T + \pi$. Using elements (1,4) and (2,4) of LHS and RHS of Eq. (2) with $\theta_4 = 0$, we find θ_6

$$\theta_6 = \text{atan2}(-(p_x' + l_{A4}), -p_y')$$

To determine θ_5 and θ_3 from θ_T, we again keep the current value of θ_3 unchanged, and θ_5 is evaluated from θ_T as $\theta_5 = \theta_3 - \theta_T$. Using elements (2,1) and (2,2) of LHS and RHS of G_2 with $\theta_4 = 0$, we can find θ_1,

$$\theta_1 = \text{atan2}(C_6s_y' + S_6s_x', C_6n_y' + S_6n_x')$$

Using elements (2,1) and (2,3) of LHS and RHS of G_2 with $\theta_4 = 0$, we can find θ_2,

$$\theta_2 = \text{atan2}\left(C_6n_y' + S_6n_x', -C_1(C_6a_y' + S_6a_x')\right)$$

and if $C_1 < 0$, then $\theta_2 = \theta_2 + \pi$.

Case 3: When both $\theta_4 = 0$ and $\theta_2 = \pi$, the joint axes of joints 1, 3, and 5 are aligned with one another. In this case, the sum of the joint angles $\theta_T = \theta_1 + \theta_5 + (-\theta_3)$ is found using elements (3,1) and (3,2) of LHS and RHS of G_2 with $\theta_4 = 0$ and $\theta_2 = \pi$ as follows. θ_6 is found in the same way as done in Case 2.

$$\theta_T = \text{atan2}(-n_z', s_z') \text{ and } \theta_6 = \text{atan2}(-(p_x' + l_{A4}), -p_y')$$

To determine θ_5, θ_1 and θ_3 from θ_T, we keep the current values of θ_1 and θ_3 unchanged, and θ_5 is evaluated from θ_T as $\theta_5 = \theta_T - \theta_1 + \theta_3$.

D. Decision Equations for Multiple Solutions

The above joint solution gives 8 possible solutions for each specified set of end-effector position and orientation. Only one of the 8 multiple solutions is the desired solution. To decide which one is the desired solution within the joint-limit constraints, we define decision indicators such that their positive value indicates the desirable solution.

To verify the inverse kinematic joint solution, we use the complete $0°$ to $360°$ joint-variable space. In this case, the decision indicators can have a negative value for joint angles outside the desirable range. We determine the sign of these indicators using the following decision equations, thereby selecting a proper IK-joint solution to use,

$$\text{KNEE} = \text{sign}(\mathbf{z}_3 \cdot (\mathbf{x}_3 \times \mathbf{x}_4)) = \text{sign}(S_4)$$
$$\text{HIP} = \text{sign}(\mathbf{z}_1 \cdot (\mathbf{x}_1 \times \mathbf{x}_2)) = \text{sign}(S_2)$$
$$\text{ANKLE} = \text{sign}(\mathbf{p}' \cdot \mathbf{x}_5) = \text{sign}(C_{5\psi}),$$

where $\mathbf{x}_i$, $\mathbf{y}_i$, and $\mathbf{z}_i$ represent the unit vectors along the principal axes of the coordinate frame i, $\mathbf{p}' = \mathbf{p} - l_{L5}\mathbf{x}_6$, and $\mathbf{p}$ is the position vector of the transformation matrix shown in Eq. (1), $\psi = \text{atan2}(S_4l_{L3}, C_4l_{L3} + l_{L4})$, and the sign function is defined as:

$$\text{sign}(x) = \begin{cases} +1, & \text{if } x \geq 0; \\ -1, & \text{if } x < 0. \end{cases}$$

Similarly, decision equations are obtained for the arm,

$$\text{SHOULDER} = \text{ARM} \cdot \text{sign}(\mathbf{z}_1 \cdot (\mathbf{x}_1 \times \mathbf{x}_2)) = \text{ARM} \cdot \text{sign}(S_2),$$
$$\text{ELBOW} = \text{sign}(\mathbf{z}_3 \cdot (\mathbf{x}_3 \times \mathbf{x}_4)) = \text{sign}(S_4)$$
$$\text{WRIST} = \text{ARM} \cdot \text{sign}(\mathbf{x}_4 \cdot \mathbf{x}_5) = \text{ARM} \cdot \text{sign}(C_5)$$

where ARM is $+1$ for a right arm and -1 for a left arm.

IV. APPLICATIONS TO OTHER HUMANOID ROBOTS

We have applied the above closed-form joint solution to other existing humanoid robots shown in Fig. 4 to illustrate the generality of our joint solution.

HOAP-2 Humanoid Robot. Comparing the kinematic structure of a HOAP-2 robot with a Hubo robot, the kinematic configuration of the leg joints is exactly the same in both robots. Hence, the above leg joint solution can be applied with the geometric link parameters from HOAP-2 robot. The arms also have the same kinematic structure except that the HOAP-2 robot has only four DOFs; it does not have joints 5 and 6. Hence, we can apply the same joint solution for the first 4 joints and putting $\theta_6 = 90°$ and $\theta_5 = 0$ in the arm equations in finding the first four joint solution.

HRP-2 Humanoid Robot. The kinematic configuration of the leg joints of an HRP-2 robot is similar to that of a Hubo robot, with the only difference being that it has an offset d_3 between link coordinate frames 2 and 3. This difference results in a small change in the link transformation matrix $^2\mathbf{A}_3$. The modifications change the joint solution slightly for θ_4, θ_5 and θ_6. For the joint configuration of the arms of an HRP-2 robot, the only difference is that the joint axis of joint 6 is rotated $90°$ as compared to that of a Hubo robot. This can be easily taken into account by adding $90°$ to θ_5.

ASIMO Humanoid Robot. The kinematic configuration of an ASIMO robot is the same as a Hubo robot except that the joint axis of joint one of both arms is slightly tilted upwards by an angle α. This modifies the transformation matrix $^{B1}\mathbf{A}_0$, which has all constant entries and is independent of joint angles. Multiplying $[\mathbf{n}, \mathbf{s}, \mathbf{a}, \mathbf{p}]$ with $^{B1}\mathbf{A}_0$ results in a modified $[\mathbf{n}, \mathbf{s}, \mathbf{a}, \mathbf{p}]$, which is then used as the input to the above joint solution for an ASIMO robot.

V. COMPUTER SIMULATIONS AND VERIFICATION

To verify the closed-form IK-joint solution, computer simulations were performed to validate the correctness of the joint solution and decision equations for a Hubo robot. Each joint angle is varied from $0°$ to $360°$ and we purposely relaxed the joint-limit constraints. For each point in the joint-variable space, forward kinematics is evaluated to obtain the position and orientation of the end-effector as in $[\mathbf{n}, \mathbf{s}, \mathbf{a}, \mathbf{p}]$. The decision equations are also evaluated to obtain the decision indicators, which identify the corresponding inverse kinematic joint solution that one should use from the available 8 joint solutions. Then the $[\mathbf{n}, \mathbf{s}, \mathbf{a}, \mathbf{p}]$ matrix and the decision indicators are fed to the inverse kinematics function, which in turn gives the joint angles from our inverse kinematic joint solution. These joint angles are compared with the values of joint angles that we have

inputed into the forward kinematics function to detect any error. Our computer simulations showed that the closed-form IK-joint solution is correct for a Hubo robot. Computer simulations were also performed to verify the correctness of the closed-form inverse kinematic joint solutions for other humanoid robots discussed in this paper.

VI. CONCLUSIONS

This paper developed a consistent methodology for deriving a closed-form joint solution of a general humanoid robot, and for a Hubo KHR-4 robot in specific. A novel reverse decoupling mechanism method was developed by viewing the kinematic chain of a limb of a humanoid robot in reverse order, decoupling it into the positioning and orientation mechanisms, and then utilizing the inverse transform technique to derive a consistent joint solution for the humanoid robot. Computer simulations have illustrated the correctness of the joint solution for a Hubo KHR-4 robot. The proposed approach has been applied to other existing humanoid robots with similar kinematic structure.

REFERENCES

[1] D. L. Pieper, "The kinematics of manipulators under computer control," Ph.D. dissertation, Stanford Univ., 1968.
[2] G. Tevatia and S. Schaal, "Inverse kinematics for humanoid robots," in *Proc. IEEE International Conference on Robotics and Automation (ICRA)*, vol. 1, 2000, pp. 294–299.
[3] M. Mistry, J. Nakanishi, G. Cheng, and S. Schaal, "Inverse kinematics with floating base and constraints for full body humanoid robot control," in *Proc. of the IEEE-RAS Intl. Conf. on Humanoid Robots*, 2008, pp. 22–27.
[4] R. Muller-Cajar and R. Mukundan, "A new algorithm for inverse kinematics," in *Proc. of the Image and Vision Computing New Zealand*, Dec. 2007, pp. 181–186.
[5] J. Wang and Y. Li, "Inverse kinematics analysis for the arm of a mobile humanoid robot based on the closed-loop algorithm," in *Proc. of the ICIA Information and Automation (ICIA)*, 2009, pp. 516–521.
[6] V. R. de Angulo and C. Torras, "Learning inverse kinematics: reduced sampling through decomposition into virtual robots," in *IEEE Transactions on Systems, Man, and Cybernetics, Part B: Cybernetics*, vol. 38, no. 6, Dec. 2008, pp. 1571–1577.
[7] K. S. Fu, R. C. Gonzalez, and C. S. G. Lee, *Robotics: Control, Sensing, Vision, and Intelligence*. McGraw-Hill, 1987.
[8] J. I. Zannatha and R. C. Limon, "Forward and inverse kinematics for a small-sized humanoid robot," in *Proc. of the IEEE Intl. Conf. on Electrical, Communications, and Computers*, 2009, pp. 111–118.
[9] D. Tolani, A. Goswami, and N. I. Badler, "Real-Time Inverse Kinematics Techniques for Anthropomorphic Limbs," *Graphical Models and Image Processing*, vol. 62, no. 5, pp. 353–388, Sep. 2000.
[10] T. Asfour and R. Dillmann, "Human-like motion of a humanoid robot arm based on a closed-form solution of the inverse kinematics problem," in *Proc. of the IEEE/RSJ Intl. Conf. on Intelligent Robots and Systems (IROS)*, 2003.
[11] T. Zhao, J. Yuan, M.-y. Zhao, and D.-l. Tan, "Research on the Kinematics and Dynamics of a 7-DOF Arm of Humanoid Robot," in *Proc. of the IEEE Intl. Conf. on Robotics and Biomimetics (ROBIO)*, Dec. 2006, pp. 1553–1558.
[12] R. P. Paul, B. E. Shimano, and G. Mayer, "Kinematic control equations for simple manipulators," in *IEEE Transactions on Systems, Man and Cybernetics*, vol. 11, 1981, pp. 449–455.
[13] Y. Cui, P. Shi, and J. Rua, "Kinematics analysis and simulation of a 6-dof humanoid robot manipulator," in *Proc. of the IEEE Intl. Asia Conf. on Informatics in Control, Automation and Robotics (CAR)*, vol. 2, Mar 2010, pp. 246–249.
[14] J. Denavit and R. S. Hartenberg, "A kinematic notation for lower-pair mechanisms based on matrices," *Trans ASME Journal of Applied Mechanisms*, vol. 23, pp. 215–221, 1955.